

# Journal of Materials Chemistry B

Materials for biology and medicine

[rsc.li/materials-b](http://rsc.li/materials-b)



ISSN 2050-750X



ROYAL SOCIETY  
OF CHEMISTRY

## COMMUNICATION

Shlomo Magdassi, Qi Ge *et al.*

Highly stretchable hydrogels for UV curing based high-resolution multimaterial 3D printing



## Highly stretchable hydrogels for UV curing based high-resolution multimaterial 3D printing†

Cite this: *J. Mater. Chem. B*, 2018, 6, 3246Received 12th March 2018,  
Accepted 3rd April 2018

DOI: 10.1039/c8tb00673c

rsc.li/materials-b

Biao Zhang,<sup>‡a</sup> Shiya Li,<sup>‡a</sup> Hardik Hingorani,<sup>‡a</sup> Ahmad Serjoui,<sup>ib</sup> Liraz Larush,<sup>b</sup> Amol A. Pawar,<sup>b</sup> Wei Huang Goh,<sup>a</sup> Amir Hosein Sakhaei,<sup>a</sup> Michinao Hashimoto,<sup>a</sup> Kavin Kowsari,<sup>a</sup> Shlomo Magdassi<sup>ib</sup>\*<sup>bc</sup> and Qi Ge<sup>ib</sup>\*<sup>ad</sup>

We report a method to prepare highly stretchable and UV curable hydrogels for high resolution DLP based 3D printing. Hydrogel solutions were prepared by mixing self-developed high-efficiency water-soluble TPO nanoparticles as the photoinitiator with an acrylamide-PEGDA (AP) based hydrogel precursor. The TPO nanoparticles make AP hydrogels UV curable, and thus compatible with the DLP based 3D printing technology for the fabrication of complex hydrogel 3D structures with high-resolution and high-fidelity (up to 7  $\mu\text{m}$ ). The AP hydrogel system ensures high stretchability, and the printed hydrogel sample can be stretched by more than 1300%, which is the most stretchable 3D printed hydrogel. The printed stretchable hydrogels show an excellent biocompatibility, which allows us to directly 3D print biostructures and tissues. The great optical clarity of the AP hydrogels offers the possibility of 3D printing contact lenses. More importantly, the AP hydrogels are capable of forming strong interfacial bonding with commercial 3D printing elastomers, which allows us to directly 3D print hydrogel-elastomer hybrid structures such as a flexible electronic board with a conductive hydrogel circuit printed on an elastomer matrix.

## Introduction

Hydrogels, hydrophilic networks of polymeric chains capable of retaining a large amount of water, have been widely used in a variety of applications including drug delivery,<sup>1,2</sup> tissue

engineering,<sup>3,4</sup> and others.<sup>5–9</sup> Additionally, recent advances in highly stretchable hydrogels have extended their applications into the fields of soft robotics,<sup>10,11</sup> transparent touch panels<sup>12</sup> and other applications requiring large deformation.<sup>13,14</sup> However, traditional fabrication methods, which mainly rely on molding and casting, confine the scope of applications due to the limited geometric complexity and the relatively low fabrication resolution.<sup>15,16</sup> Along with recent rapid developments in 3D printing, various attempts have also been made to use 3D printing to fabricate hydrogel structures with complex geometries including vascular networks,<sup>17,18</sup> porous scaffolds,<sup>19</sup> meniscus substitutes<sup>20</sup> and others.<sup>21–23</sup> Among all the existing 3D printing technologies, extrusion-based direct ink writing is most widely adopted as it only requires the hydrogel precursor to exhibit a shear thinning effect at a critical shear rate, which can be readily controlled by adding viscous additives such as nanoclay<sup>24,25</sup> and natural polymers<sup>26</sup> into a wide range of hydrogel precursors including not only the widely used monomers and crosslinkers such as poly(ethylene glycol)diacrylate (PEGDA),<sup>27</sup> acrylamide (AAm),<sup>20</sup> and *N*-isopropylacrylamide (NIPAM)<sup>28</sup> (Fig. 1a), but also natural polymers or their derivatives such as alginate,<sup>29,30</sup> hyaluronic acid (HA),<sup>31</sup> nanofibrillated cellulose (NFC),<sup>28</sup> gelatin (Gel)<sup>32–34</sup> and gelatin methacrylate (GelMA)<sup>35</sup> to enhance the hydrogel's mechanical performance, *i.e.* increasing the stretchability of the printed hydrogels to 1000%<sup>20</sup> (Fig. 1a). However, the manner of directly writing 3D structures by extruding printing ink through a printing nozzle with  $\sim 100$  microns diameter limits the geometric complexity to 2.5 dimensional or simple 3D structures, and the printing resolution to a hundred micron scale (Fig. 1b), which is insufficient for applications such as 3D printed tissue substitutes which require high-fidelity replicas to limit mismatch during transplantation.<sup>20</sup> Moreover, although extrusion-based multimaterial 3D printing approaches have been developed by adding extra printing nozzles to fabricate multimaterial 3D hydrogel structures, the demonstrated examples are limited to multimaterial structures that are made of hydrogels from one material family with different compositions<sup>36,37</sup> or with different added dyes.<sup>38</sup>

<sup>a</sup> Digital Manufacturing and Design Centre, Singapore University of Technology and Design, 487372, Singapore. E-mail: ge\_qi@sutd.edu.sg

<sup>b</sup> Casali Centre for Applied Chemistry, Institute of Chemistry, The Centre for Nanoscience and Nanotechnology, The Hebrew University of Jerusalem, Jerusalem 9190401, Israel. E-mail: magdassi@mail.huji.ac.il

<sup>c</sup> Singapore-HUJ Alliance for Research and Enterprise, Energy and Energy-water Nexus Research Group, Campus for Research Excellence and Technological Enterprise, 138602, Singapore

<sup>d</sup> Science and Math Cluster, Singapore University of Technology and Design, 487372, Singapore

† Electronic supplementary information (ESI) available. See DOI: 10.1039/c8tb00673c

‡ These authors contributed equally to this work.

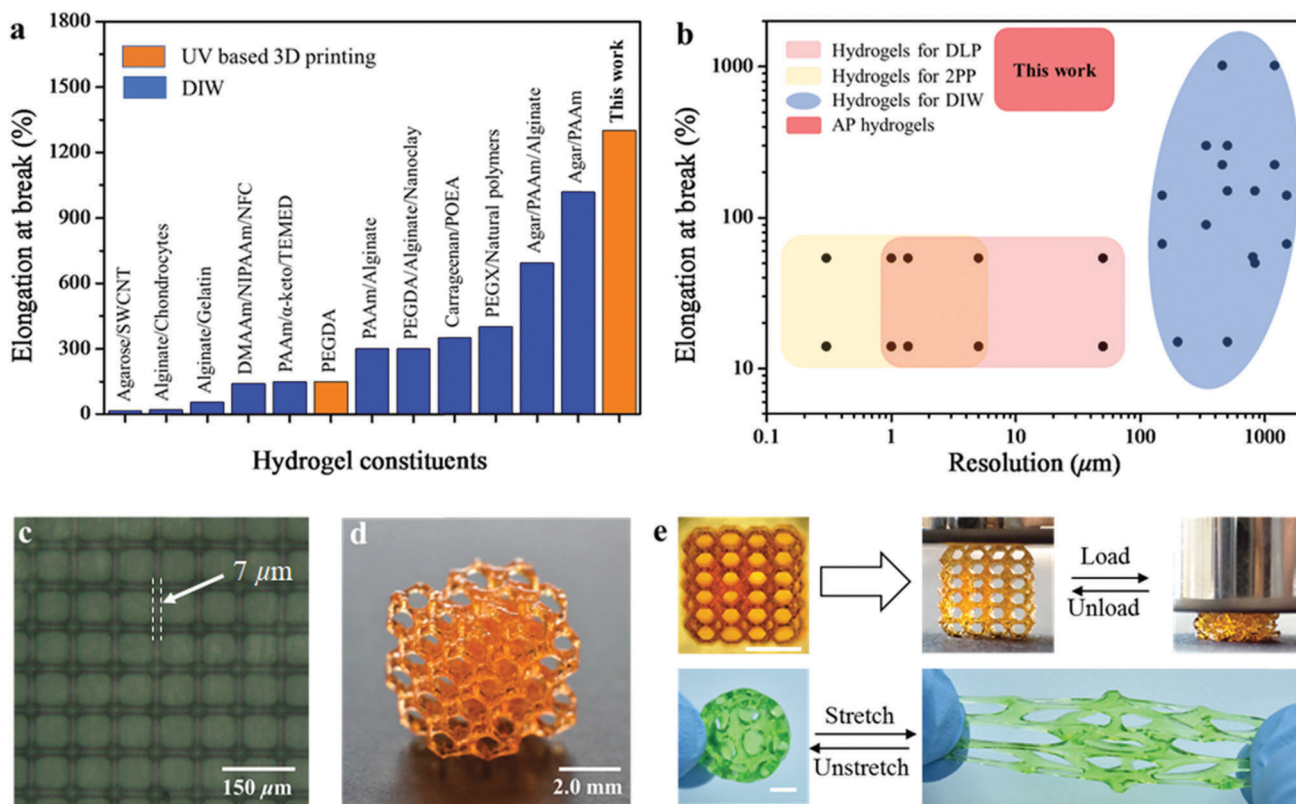


**Fig. 1** Highly stretchable hydrogels for UV curing based 3D printing. (a) Comparison of the stretchabilities of the 3D printable hydrogels reported in previous studies and this work (see details in Fig. S1 and Table S1, ESI†). (b) The stretchability–printing resolution relation suggests that the hydrogels developed in this work are not only highly stretchable but also compatible with high resolution 3D printing. The black dots represent the break strains which were reported by previous works (see details in Fig. S1 and Table S1, ESI†). (c) 3D printed high resolution hydrogel grid. (d) 3D printed hydrogel Kelvin form. (e) Demonstrations of the highly stretchable 3D printed hydrogel structures: the upper pictures presenting a Kelvin hydrogel form capable of sustaining a large compressive deformation; the bottom part presents a 3D printed hydrogel bucky ball under a large stretching deformation (scale bar: 2 mm).

UV curing based 3D printing techniques that transform a liquid polymer resin into solid 3D structures *via* localized photopolymerization controlled by high-precision UV irradiation have been adopted to fabricate hydrogel structures requiring high printing resolution and high geometric complexity.<sup>39–49</sup> The most commonly used UV based 3D printing techniques for hydrogel 3D printing include two-photon polymerization (2PP), which has been applied to fabricate high resolution structures with  $\sim 100$  nm features used in tissue engineering, biosensors, drug delivery systems, and others<sup>47,48</sup> (Fig. 1b); and digital light processing (DLP) based 3D printing, which employs the digital mask projection to trigger localized photo-polymerization, and enables fast fabrication of 3D hydrogel structures with feature sizes ranging from 1  $\mu\text{m}$  to 100  $\mu\text{m}$ <sup>39–42,44–46,49</sup> (Fig. 1b). Furthermore, with the addition of efficient material exchange mechanisms, multimaterial DLP 3D printing systems have been developed to fabricate multimaterial functional structures.<sup>50,51</sup> In general, UV based hydrogel 3D printing takes place in an aqueous solution, which requires all the constituents including monomers, crosslinkers, and photoinitiators to be highly water-soluble. However, due to the absence of highly efficient water-soluble photoinitiators, most of the current protocols for UV based hydrogel 3D printing use nonefficient, poorly water-soluble photoinitiators, which require substantial agitation and/or heating

or mixing with organic solvents to obtain clear precursor solutions.<sup>52,53</sup> The polymers currently used for UV based hydrogel 3D printing are limited to PEGDA and poly(*N*-isopropylacrylamide) (pNIPAM) which are relatively brittle (the break strain is less than 100%, Fig. S1 in the ESI†)<sup>42,49</sup> and are not sufficient for many applications that require large deformation.<sup>42,53</sup> Therefore, a general method to prepare highly stretchable hydrogels that are UV curable, and thus suitable for DLP based high resolution 3D printing, is still a critical demand and central challenge in the field of 3D printing hydrogels.

Here, we present a novel but simple method to prepare highly stretchable and UV curable hydrogels for DLP and other UV curing based 3D printing approaches. Hydrogel precursors are prepared by mixing an acrylamide–PEGDA (AP) mixture with a self-developed highly water-soluble, high-efficiency photoinitiator, 2,4,6-trimethylbenzoyl-diphenylphosphine oxide (TPO) nanoparticles. We choose acrylamide as the monomer as it has been found to form highly stretchable hydrogels,<sup>54</sup> and use PEGDA as the crosslinker to tune the crosslinking density and the mechanical performance of the hydrogel system. The water-soluble TPO nanoparticles enable us to prepare high water content (50–80%) hydrogel precursors. AP hydrogels are UV curable, and thus compatible with DLP based 3D printing, which allows us to fabricate hydrogel 3D structures with high

resolutions (up to 7  $\mu\text{m}$ , Fig. 1c) and complex geometries (Fig. 1d) (details about hydrogel 3D printing are presented in the ESI†). The AP hydrogel system exhibits high stretchability (Fig. 1e, Movie S1 in the ESI†), and a printed hydrogel sample can be stretched by up to 1300%, which, to our best knowledge, is the most stretchable 3D printed hydrogel sample. Moreover, the strong interfacial bonding between the AP hydrogels and commercial 3D printing elastomers enables multimaterial 3D printing to fabricate hydrogel–elastomer hybrid structures.

## Results and discussion

As depicted in Fig. 2a, we prepared an acrylamide–PEGDA (AP) hydrogel precursor by mixing acrylamide as the monomer, poly(ethylene glycol)diacrylate (PEGDA) as the crosslinker, and self-developed highly water-soluble 2,4,6-trimethylbenzoyl-diphenylphosphine oxide (TPO) nanoparticles<sup>44</sup> as the photoinitiator into water (water content: 50–80 wt%). We chose TPO as it has been claimed to be one of the most efficient commercially available photoinitiators.<sup>55,56</sup> However, due to the low water solubility (3.13 mg L<sup>-1</sup> at 25 °C),<sup>44</sup> we converted the as-purchased TPO powders into highly water-soluble TPO nanoparticles. As shown in Fig. 2b, the idea of imparting water-solubility to TPO is to encapsulate TPO powders within commercially available surfactants, sodium dodecyl sulfate (SDS) containing a hydrophilic head and a hydrophobic tail. In addition, polyvinylpyrrolidone (PVP) is used as a crystallization inhibitor. After spray-drying the prepared oil-in-water microemulsions containing TPO, highly water-soluble TPO nanoparticles are produced (details about the preparation of TPO nanoparticles are presented in Fig. S2, ESI†). In Fig. 2c, dissolving 5 wt% TPO nanoparticles in water results in a clear transparent system (the right vial). In comparison, the as-purchased TPO powders are not water-soluble at all (the left vial).

During 3D printing, patterned UV radiation provided by a digital micromirror device stimulates localized photopolymerization

by opening the double bonds on the acrylate functional groups on both the acrylamide and PEGDA to form permanently crosslinked networks (Fig. 2a) and solidify the polymer solution into the corresponding solid pattern. Layer-by-layer solidification continues until the fabrication of an entire 3D structure is complete. It should be noted that the efficiency of the photoinitiator plays a vital role as it determines the kinetics of photopolymerization and properties of the printed objects. TPO that has a high molar attenuation coefficient ( $\sim 400\text{--}600 \text{ M}^{-1} \text{ cm}^{-1}$ ) within the spectrum of 365–405 nm<sup>57</sup> is an ideal photoinitiator for UV based hydrogel 3D printing and allows us to print hydrogels at a fast rate (about 10 seconds/layer). In Fig. 2d, we compare the efficiency of TPO nanoparticles with that of the commercially available, water-soluble photoinitiator, Irgacure 2959 (I2959) (Sigma Aldrich, MO, United States), which is most commonly used in aqueous photocurable systems and has been widely used for 3D printing hydrogels.<sup>42,43,58</sup> The polymerization kinetics tests reveal that an AP hydrogel solution prepared with 80 wt% water and a 20 wt% acrylamide–PEGDA mixture with a PEGDA(700)/acrylamide mixing ratio of 0.625 wt% (PEGDA(700) refers to the PEGDA with a molecular weight of 700 g mol<sup>-1</sup>), and a TPO nanoparticles/acrylamide mixing ratio of 0.5 wt%, requires 1 min to achieve 90% polymerization. In contrast, although I2959 has been used to successfully 3D print hydrogel structures made of pure PEGDA,<sup>42</sup> Fig. 2d suggests that it fails in the gelation of the AP hydrogel as the degree of polymerization is saturated at less than 10% (details about the efficiency investigation of TPO nanoparticles are presented in Fig. S3, ESI†).

The AP hydrogel system exhibits a high tailorability of mechanical performance by tuning the material parameters including the concentration and molecular weight of PEGDA as well as the water content. In Fig. 3a, the stress–stretch curve shows that a hydrogel sample made of 80 wt% water and a 20 wt% acrylamide–PEGDA mixture with a PEGDA(700)/acrylamide mixing ratio of 0.625 wt% exhibits large deformation, and it can be elongated to more than thirteen times its original length. In Fig. 3b, the increase in the concentration of PEGDA(700) results in a decrease in the stretchability, but an increase in the hydrogel's stiffness as more PEGDA molecules lead to higher crosslinking density but reduce the average chain length between crosslinking points, which undermines the hydrogel's stretchability.<sup>50</sup> Alternatively, the mechanical performance can be adjusted using PEGDAs with different molecular weights. Fig. 3c shows that the hydrogel's stretchability is increased using PEGDA with higher molecular weight, which also results in the decline in the stiffness of the hydrogel. Moreover, the water content has a significant impact on the mechanical performance. In Fig. 3d, the stretchability of an AP hydrogel that is made of 0.625 wt% PEGDA(700)/acrylamide increases from  $\sim 5$  to  $\sim 13$ , while the stiffness decreases from  $\sim 260$  kPa to  $\sim 7$  kPa when the water content is increased from 50% to 80% (see details about uniaxial tensile tests on AP hydrogels in Fig. S4, ESI†).

Besides the effects on the mechanical performance, the material parameters also affect the curing time, which is one

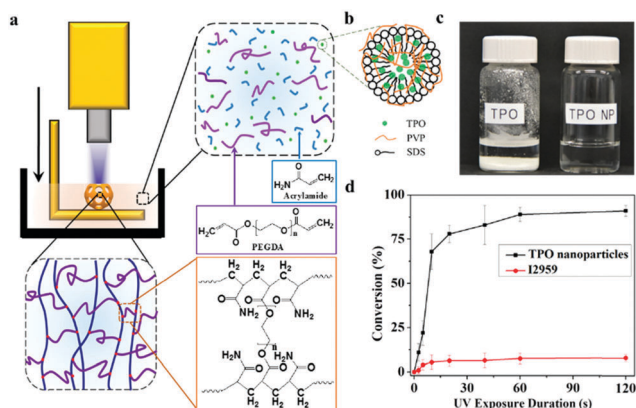


Fig. 2 AP hydrogels for DLP based 3D printing. (a) The 3D printing process and chemical structures of acrylamide, PEGDA and the formed crosslinking network upon UV exposure. (b) Schematic of TPO nanoparticles. (c) Comparison of the water solubilities of the as-purchased TPO powders (5 wt%, left) and TPO nanoparticles (5 wt%, right) in water. (d) Comparison of the polymerization kinetics of TPO nanoparticles and I2959.

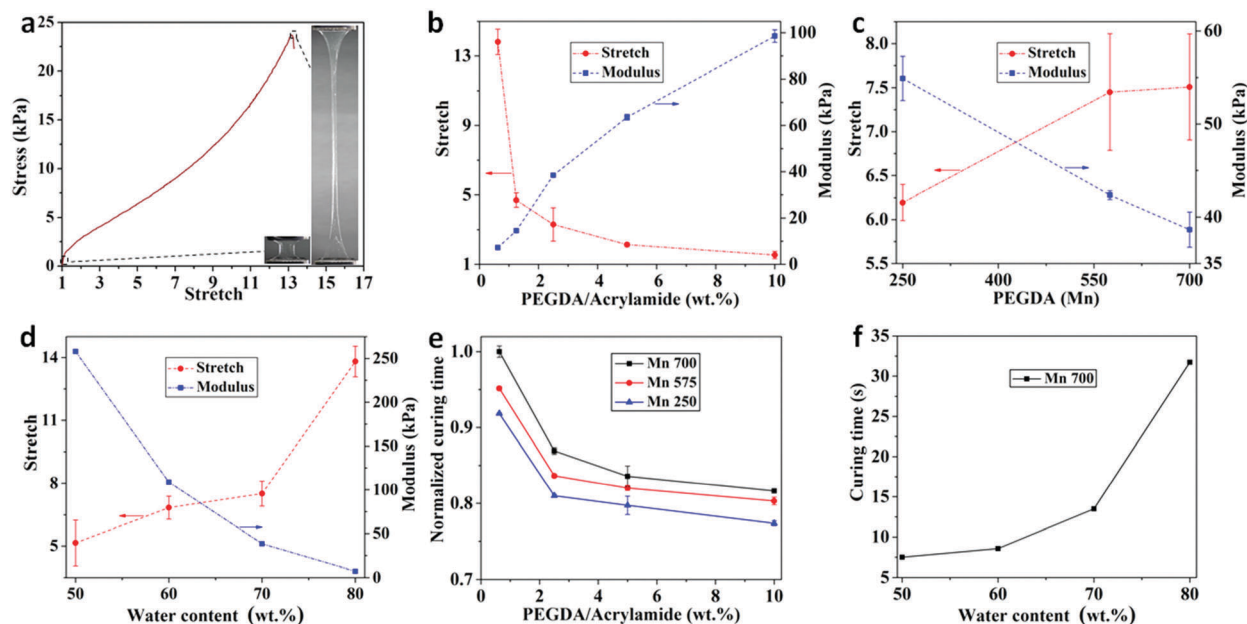


Fig. 3 Effects of material parameters on the mechanical performance and the 3D printing process. (a) The stress–stretch curve showing that a hydrogel sample can be elongated to more than thirteen times its original length. (b) The effect of the concentration of PEGDA on the mechanical performance. (c) The effect of the molecular weight of PEGDA on the mechanical performance. (d) The effect of the water content on the mechanical performance. (e) The effects of PEGDA on the curing time. (f) The effect of the water content on the curing time.

of the key parameters in the 3D printing process. As shown in Fig. 3e, the increase in the PEGDA concentration results in the reduction of the curing time, and the PEGDA with larger molecular weight requires longer UV exposure. In addition, the effect of water content on the curing time is remarkable. The time required to cure a 140  $\mu\text{m}$  thick layer for the AP hydrogel consisting of 0.625 wt% PEGDA(700)/acrylamide and 0.5 wt% TPO nanoparticles/acrylamide increases significantly from 7.5 s to 32 s with the increase of the water content from 50% to 80%. Besides, we also investigated the effects of various dyes which are used to improve the printing resolution.<sup>43,59</sup> Generally, when more dyes are added, a longer time for curing the same layer thickness is needed (see details about curing time characterization in Fig. S5, ESI<sup>†</sup>). Overall, the curing time to print a 140  $\mu\text{m}$  thick layer in this study is within a reasonably short time period (less than 30 s). Therefore, the AP hydrogel system is ideal for DLP and other UV curing based high resolution 3D printing approaches.

The compatibility with the DLP 3D printing technology empowers the AP hydrogel to fabricate 3D structures that not only possess complex geometries, but also exhibit large deformation. In Fig. 4a, we investigated the deformability of a lattice structure printed with the AP hydrogel through a uniaxial tensile test (see details about mechanical tests on a hydrogel lattice structure in Fig. S6, ESI<sup>†</sup>). Before the failure, the lattice structure was elongated to five times its original height (Fig. 4b(i) and (ii)). Finally, the breaking occurred at one corner of the lattice (Fig. 4b(iii), Movie S3, ESI<sup>†</sup>). We also performed Finite Element (FE) simulations to study the local deformation distributions (details about FE simulations are presented in Fig. S7, ESI<sup>†</sup>). In Fig. 4c, a maximum principal strain of  $\sim 310\%$

is observed at the middle intersections when the lattice is stretched by five times.

The compatibility with the high-resolution 3D printing and the excellent mechanical performance make AP hydrogels ideal materials to fabricate tissue substitutes such as menisci,<sup>20</sup> vascular grafts,<sup>60,61</sup> and tracheal splints.<sup>59</sup> In these tissue engineering applications, the biocompatibility is vital. To examine the biocompatibility of AP hydrogels with different dyes (red food colouring and Sudan I), we performed a cell viability assay over a 7 day cell culture period. NIH-3T3 fibroblast cells and HepG2 liver cancer cells were cultured in individual cell culture wells that contained the printed hydrogels (see details in the ESI<sup>†</sup>). The cell viability was sustained above 93% over a 7 day culture period for the hydrogels with different dyes (Fig. 4d and e). The high cell viability over prolonged cell culture suggests that the printed hydrogels do not exhibit toxic effects on cells resulting in cell death.

The excellent biocompatibility allows us to use AP hydrogels to directly 3D print biostructures and tissues, *i.e.*, ears, noses, and stretchable blood vessels (Movie S4, ESI<sup>†</sup>), as shown in Fig. 4f. Furthermore, as the wavelength of the light source we used is 405 nm, higher than the UV-B band, *i.e.* 315 nm, which has been reported to induce serious DNA damage and apoptosis,<sup>62,63</sup> AP hydrogels also possess a great visible light transparency. Fig. 4g and h present the light transmittance over the light spectrum from 250 nm to 850 nm (see details in the ESI<sup>†</sup>). AP hydrogels with different concentrations of PEGDA (Fig. 4g) and water contents (Fig. 4h) are highly transparent with the visible light transmittance above 90%. In the UV region (below 400 nm), the light transmittance decreases drastically due to UV light absorption by the TPO nanoparticles and partly by

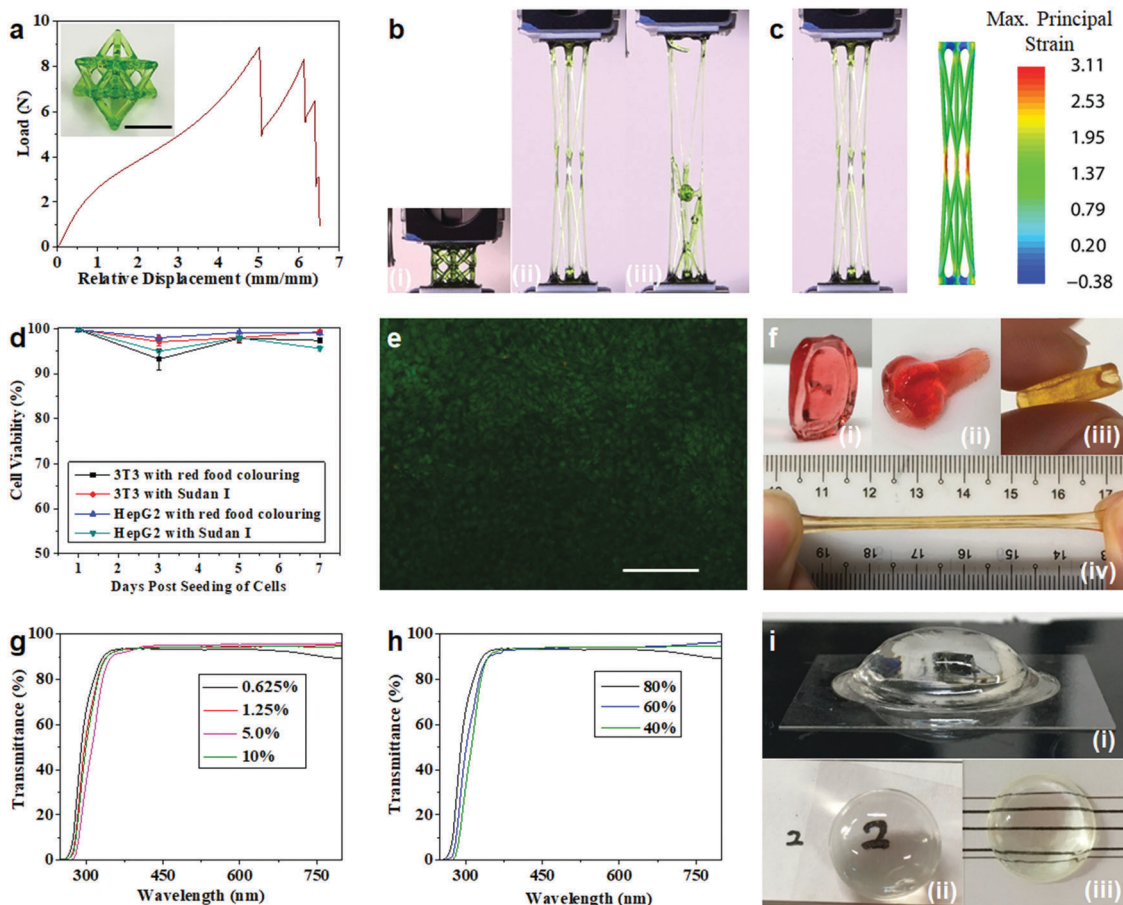


**Fig. 4** 3D printed hydrogel structures with complex geometries and superior performances. (a) The result of the uniaxial tensile test of a printed hydrogel lattice structure (the scale bar in the inset is 10 mm). (b) The snapshots of the uniaxial tensile tests: (i) before the test starts; (ii) right before the rupture; and (iii) the first rupture occurs at one corner of the lattice structure. (c) The comparison between the experiment and FE simulation. (d) The results of cell viability tests. (e) Live/dead assay on day 7 post seeding of NIH-3T3 cells cultured with a hydrogel slab. (f) 3D printed tissues: (i) an ear; (ii) a nose; (iii) a blood vessel; and (iv) a largely stretched blood vessel (Movie S4, ESI<sup>†</sup>). (g) The transmittance results of the hydrogels made of 80 wt% water and different PEGDA(700)/acrylamide mixing ratios. (h) The transmittance results of the hydrogels made of a PEGDA(700)/acrylamide mixture with a mixing ratio of 0.625% and different water contents. (i) 3D printing optical lenses using the AP hydrogel: (i) the side view of a printed lens; and (ii) and (iii) the optical effects of the printed lens.

the oligomer.<sup>64</sup> The remarkable visible light transmittance makes the AP hydrogels ideal for 3D printing of optical components. Fig. 4i demonstrates a 3D printed convex lens made of an AP hydrogel containing 50 wt% water and a 50 wt% acrylamide-PEGDA mixture with a PEGDA(700)/acrylamide mixing ratio of 0.625 wt%, which shows reasonably good optical performance and offers the possibility of 3D printing contact lenses.<sup>65</sup>

The robust bonding of hydrogels to elastomers is desired to develop hydrogel-elastomer hybrids which can be used to develop stretchable electronics, hydrogel soft robots, and stretchable diffusive and reactive microfluidic chips.<sup>10,13,66</sup> However, 3D printable hydrogels that are capable of forming strong bonding with other 3D printable elastomers have not yet been achieved. In Fig. 5a and b, we demonstrate that the AP hydrogel forms strong interfacial bonding with a commercial 3D printing acrylate based elastomer (TangoPlus, Stratays, MN, United States) in a uniaxial tensile test. The hydrogel-elastomer hybrid sample was prepared using a customized multimaterial 3D printing system<sup>50,51</sup> (see details in the ESI<sup>†</sup>). During loading, as the acrylate elastomer is

about 100 times stiffer than the hydrogel (Fig. 5c), most deformation occurs on the hydrogel. The fact that the composite breaks in the hydrogel region rather than at the interface, after being stretched by 4.5 times (Movie S5, ESI<sup>†</sup>), suggests that the interface between the AP hydrogel and the acrylate elastomer is reasonably tough. We attribute the strong interfacial bonding to covalent bonds between the hydrogels and the elastomer (Fig. S9, ESI<sup>†</sup>).<sup>13</sup> During printing, the surface of the printed elastomer still has unreacted acrylate-based monomers, which covalently bond the unreacted double bonds on acrylamide or PEGDA in the hydrogel precursor upon UV irradiation. This allows us to print hydrogel-elastomer multimaterial structures and devices in a variety of applications. Fig. 5d presents a multimaterial printed hydrogel sheet with the embedded “SUTD” letters that are made of the TangoPlus elastomer. The strong interfacial bonding avoids the debonding between the hydrogel matrix and the “SUTD” elastic letters even under large deformation (Movie S6, ESI<sup>†</sup>). The capability of printing hydrogel-elastomer hybrids will significantly simplify the process of fabricating conductive hydrogel based flexible electronics.<sup>13</sup> As shown in Fig. 5e,

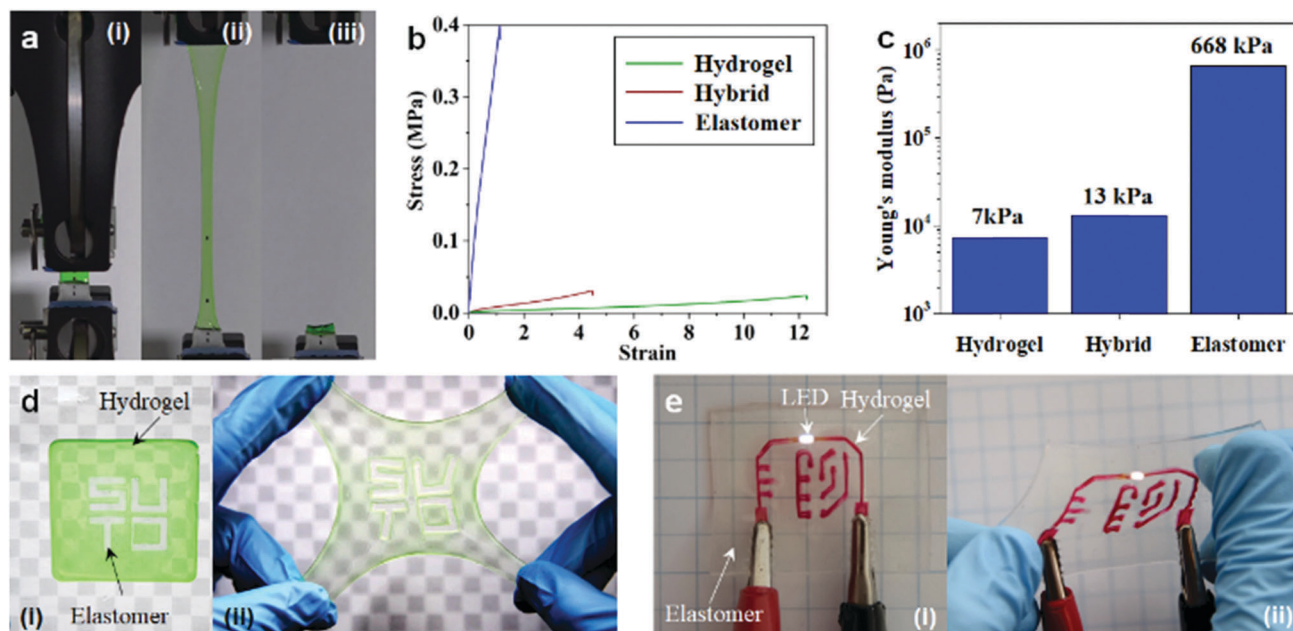


Fig. 5 Multimaterial 3D printing between hydrogels and elastomers. (a) The snapshots of the uniaxial tensile test on a hydrogel–elastomer hybrid specimen: (i) before the test; (ii) right before the rupture; and (iii) after the rupture. (b) The stress–strain curves of a pure hydrogel sample, a pure 3D printing elastomer, and a hydrogel–elastomer hybrid. (c) The Young's moduli extracted from the stress–strain curves. (d) A 3D printed multimaterial hydrogel sheet with the embedded “SUTD” letters under large deformation. (e) A highly stretchable electronic board realized by printing an ionic hydrogel circuit on an elastomeric substrate.

we demonstrate the functionality of a printed hydrogel circuit on an elastomeric substrate by lighting up an LED with an a.c. power source connected to the hydrogel circuit. The ionic conductivity is achieved by adding lithium chloride to the hydrogel solution.<sup>14</sup> The conductive hydrogel circuit can indeed maintain its electrical functionality even under severe deformation (Movie S7, ESI<sup>†</sup>).

## Conclusions

In summary, we present a simple but versatile method to prepare highly stretchable and UV curable hydrogels for the DLP and other UV curing based 3D printing technologies. The AP hydrogel system ensures high stretchability, and the printed hydrogel sample can be stretched to more than thirteen times its original length. The compatibility with the DLP 3D printing technology enables the fabrication of complex 3D hydrogel structures with high-resolution and high-fidelity. The AP hydrogel system exhibits a high tailorability of mechanical performance which can be easily adjusted by tuning the concentration and molecular weight of PEGDA as well as the water content on the mechanical performance. The AP hydrogels show an excellent biocompatibility which allows us to directly 3D print biostructures and tissues. More importantly, the AP hydrogels are capable of forming strong interfacial bonding with commercial 3D printing elastomers, which allows us to directly 3D print hydrogel–elastomer hybrid structures such as a flexible electronic board with a conductive hydrogel circuit printed on an elastomer matrix.

## Author contributions

B. Z., S. L., H. H., A. S., and Q. G. conceived the idea and designed the research. S. L. and H. H. printed the hydrogel

structures. B. Z., S. L., H. H., and A. S. performed the experiments. K. K. assisted with the experiments. S. L., H. M. and W. H. G. designed and conducted the cell viability tests. L. L., A. A. P., and S. M. prepared the water-soluble TPO nanoparticles. B. Z., S. L. and Q. G. drafted the manuscript and all authors contributed to the writing of the manuscript.

## Conflicts of interest

There are no conflicts to declare.

## Acknowledgements

Biao Zhang, Shiya Li, Hardik Hingorani, Ahmad Serjouei, Wei Huang Goh, Amir Hosein Sakhaei, Michinao Hashimoto, Kavin Kowsari, and Qi Ge acknowledge the financial support from the SUTD Digital Manufacturing and Design Centre (DMand), supported by the Singapore National Research Foundation. Qi Ge acknowledges the Startup Research Grant (SRG) from the Singapore University of Technology and Design. Shlomo Magdassi acknowledges the support by a grant from the National Research Foundation, Prime Minister's Office, Singapore, under its Campus of Research Excellence and Technological Enterprise (CREATE) programme.

## References

- 1 Y. Qiu and K. Park, *Adv. Drug Delivery Rev.*, 2001, **53**, 321.
- 2 R. Langer, *Science*, 1990, **249**, 1527.
- 3 G. D. Nicodemus and S. J. Bryant, *Tissue Eng., Part B*, 2008, **14**, 149.

- 4 S. Ladet, L. David and A. Domard, *Nature*, 2008, **452**, 76.
- 5 X. Ma, X. Qu, W. Zhu, Y.-S. Li, S. Yuan, H. Zhang, J. Liu, P. Wang, C. S. E. Lai, F. Zanella, G.-S. Feng, F. Sheikh, S. Chien and S. Chen, *Proc. Natl. Acad. Sci. U. S. A.*, 2016, **113**, 2206.
- 6 Y. Takashima, S. Hatanaka, M. Otsubo, M. Nakahata, T. Kakuta, A. Hashidzume, H. Yamaguchi and A. Harada, *Nat. Commun.*, 2012, **3**, 1270.
- 7 P. Calvert, *Adv. Mater.*, 2009, **21**, 743.
- 8 N. A. Peppas, J. Z. Hilt, A. Khademhosseini and R. Langer, *Adv. Mater.*, 2006, **18**, 1345.
- 9 L. Dong, A. K. Agarwal, D. J. Beebe and H. Jiang, *Nature*, 2006, **442**, 551.
- 10 H. Yuk, S. Lin, C. Ma, M. Takaffoli, N. X. Fang and X. Zhao, *Nat. Commun.*, 2017, **8**, 14230.
- 11 C. Larson, B. Peele, S. Li, S. Robinson, M. Totaro, L. Beccai, B. Mazzolai and R. Shepherd, *Science*, 2016, **351**, 1071.
- 12 C.-C. Kim, H.-H. Lee, K. H. Oh and J.-Y. Sun, *Science*, 2016, **353**, 682.
- 13 H. Yuk, T. Zhang, G. A. Parada, X. Liu and X. Zhao, *Nat. Commun.*, 2016, **7**, 12028.
- 14 C. Keplinger, J.-Y. Sun, C. C. Foo, P. Rothemund, G. M. Whitesides and Z. Suo, *Science*, 2013, **341**, 984.
- 15 V. Liu Tsang and S. N. Bhatia, *Adv. Drug Delivery Rev.*, 2004, **56**, 1635.
- 16 D. W. Hutmacher, *J. Biomater. Sci., Polym. Ed.*, 2001, **12**, 107.
- 17 D. B. Kolesky, R. L. Truby, A. S. Gladman, T. A. Busbee, K. A. Homan and J. A. Lewis, *Adv. Mater.*, 2014, **26**, 3124.
- 18 J. S. Miller, K. R. Stevens, M. T. Yang, B. M. Baker, D.-H. T. Nguyen, D. M. Cohen, E. Toro, A. A. Chen, P. A. Galie, X. Yu, R. Chaturvedi, S. N. Bhatia and C. S. Chen, *Nat. Mater.*, 2012, **11**, 768.
- 19 T. Billiet, E. Gevaert, T. De Schryver, M. Cornelissen and P. Dubruel, *Biomaterials*, 2014, **35**, 49.
- 20 J. Wei, J. Wang, S. Su, S. Wang, J. Qiu, Z. Zhang, G. Christopher, F. Ning and W. Cong, *RSC Adv.*, 2015, **5**, 81324.
- 21 M. S. Manno, Z. Jiang, T. James, Y. L. Kong, K. A. Malatesta, W. O. Soboyejo, N. Verma, D. H. Gracias and M. C. McAlpine, *Nano Lett.*, 2013, **13**, 2634.
- 22 T. J. Klein, S. C. Rizzi, J. C. Reichert, N. Georgi, J. Malda, W. Schuurman, R. W. Crawford and D. W. Hutmacher, *Macromol. Biosci.*, 2009, **9**, 1049.
- 23 R. Chang, J. Nam and W. Sun, *Tissue Eng., Part C*, 2008, **14**, 157.
- 24 S. Hong, D. Sycks, H. F. Chan, S. Lin, G. P. Lopez, F. Guilak, K. W. Leong and X. Zhao, *Adv. Mater.*, 2015, **27**, 4035.
- 25 H. Yuk and X. Zhao, *Adv. Mater.*, 2018, **30**, 1704028.
- 26 A. L. Rutz, K. E. Hyland, A. E. Jakus, W. R. Burghardt and R. N. Shah, *Adv. Mater.*, 2015, **27**, 1607.
- 27 S. E. Bakarich, S. Beirne, G. G. Wallace and G. M. Spinks, *J. Mater. Chem. B*, 2013, **1**, 4939.
- 28 A. S. Gladman, E. A. Matsumoto, R. G. Nuzzo, L. Mahadevan and J. A. Lewis, *Nat. Mater.*, 2016, **15**, 413.
- 29 K. Arai, Y. Tsukamoto, H. Yoshida, H. Sanae, T. A. Mir, S. Sakai, T. Yoshida, M. Okabe, T. Nikaido and M. Taya, *Int. J. Bioprint.*, 2016, **2**, 153.
- 30 K. Arai, S. Iwanaga, H. Toda, C. Genci, Y. Nishiyama and M. Nakamura, *Biofabrication*, 2011, **3**, 034113.
- 31 H. W. Kang, S. J. Lee, I. K. Ko, C. Kengla, J. J. Yoo and A. Atala, *Nat. Biotechnol.*, 2016, **34**, 312.
- 32 F. You, X. Wu and X. Chen, *Int. J. Polym. Mater.*, 2017, **66**, 299.
- 33 B. Duan, L. A. Hockaday, K. H. Kang and J. T. Butcher, *J. Biomed. Mater. Res., Part A*, 2013, **101**, 1255.
- 34 Y. He, F. Yang, H. Zhao, Q. Gao, B. Xia and J. Fu, *Sci. Rep.*, 2016, **6**, 29977.
- 35 W. Liu, Y. S. Zhang, M. A. Heinrich, F. De Ferrari, H. L. Jang, S. M. Bakht, M. M. Alvarez, J. Yang, Y. C. Li and G. Trujillo-de Santiago, *Adv. Mater.*, 2017, **29**, 1604630.
- 36 A. Nadernezhad, N. Khani, G. A. Skvortsov, B. Toprakhisar, E. Bakirci, Y. Menciloglu, S. Unal and B. Koc, *Sci. Rep.*, 2016, **6**, 33178.
- 37 A. L. Rutz, K. E. Hyland, A. E. Jakus, W. R. Burghardt and R. N. Shah, *Adv. Mater.*, 2015, **27**, 1607.
- 38 W. Liu, Y. S. Zhang, M. A. Heinrich, F. De Ferrari, H. L. Jang, S. M. Bakht, M. M. Alvarez, J. Yang, Y.-C. Li, G. Trujillo-deSantiago, A. K. Miri, K. Zhu, P. Khoshakhlagh, G. Prakash, H. Cheng, X. Guan, Z. Zhong, J. Ju, G. H. Zhu, X. Jin, S. R. Shin, M. R. Dokmeci and A. Khademhosseini, *Adv. Mater.*, 2017, **29**, 1604630.
- 39 A. P. Zhang, X. Qu, P. Soman, K. C. Hribar, J. W. Lee, S. Chen and S. He, *Adv. Mater.*, 2012, **24**, 4266.
- 40 M. Gou, X. Qu, W. Zhu, M. Xiang, J. Yang, K. Zhang, Y. Wei and S. Chen, *Nat. Commun.*, 2014, **5**, 3774.
- 41 W. Zhu, J. Li, Y. J. Leong, I. Rozen, X. Qu, R. Dong, Z. Wu, W. Gao, P. H. Chung and J. Wang, *Adv. Mater.*, 2015, **27**, 4411.
- 42 J. Warner, P. Soman, W. Zhu, M. Tom and S. Chen, *ACS Biomater. Sci. Eng.*, 2016, **2**, 1763.
- 43 Z. Wang, X. Jin, R. Dai, J. F. Holzman and K. Kim, *RSC Adv.*, 2016, **6**, 21099.
- 44 A. A. Pawar, G. Saada, I. Cooperstein, L. Larush, J. A. Jackman, S. R. Tabaei, N.-J. Cho and S. Magdassi, *Sci. Adv.*, 2016, **2**, e1501381.
- 45 W. Yang, H. Yu, W. Liang, Y. Wang and L. Liu, *Micromachines*, 2015, **6**, 1903.
- 46 C. I. A. Mandon, L. J. Blum and C. A. Marquette, *Anal. Chem.*, 2016, **88**, 10767.
- 47 A. Ovsianikov, A. Deiwick, S. Van Vlierberghe, P. Dubruel, L. Möller, G. Dräger and B. Chichkov, *Biomacromolecules*, 2011, **12**, 851.
- 48 A. I. Ciuciu and P. J. Cywiński, *RSC Adv.*, 2014, **4**, 45504.
- 49 D. Han, Z. Lu, S. A. Chester and H. Lee, *Sci. Rep.*, 2018, **8**, 1963.
- 50 Q. Ge, A. H. Sakhaei, H. Lee, C. K. Dunn, N. X. Fang and M. L. Dunn, *Sci. Rep.*, 2016, **6**, 31110.
- 51 Q. Wang, J. A. Jackson, Q. Ge, J. B. Hopkins, C. M. Spadaccini and N. X. Fang, *Phys. Rev. Lett.*, 2016, **117**, 175901.
- 52 B. D. Fairbanks, M. P. Schwartz, C. N. Bowman and K. S. Anseth, *Biomaterials*, 2009, **30**, 6702.
- 53 H. Lee, J. Zhang, H. Jiang and N. X. Fang, *Phys. Rev. Lett.*, 2012, **108**, 214304.

- 54 J.-Y. Sun, X. Zhao, W. R. K. Illeperuma, O. Chaudhuri, K. H. Oh, D. J. Mooney, J. J. Vlassak and Z. Suo, *Nature*, 2012, **489**, 133.
- 55 H. Gruber, *Prog. Polym. Sci.*, 1992, **17**, 953.
- 56 T. Sumiyoshi, W. Schnabel, A. Henne and P. Lechtken, *Polymer*, 1985, **26**, 141.
- 57 M. G. Neumann, W. G. Miranda Jr, C. C. Schmitt, F. A. Rueggeberg and I. C. Correa, *J. Dent.*, 2005, **33**, 525.
- 58 S. Lee, X. Tong and F. Yang, *Acta Biomater.*, 2014, **10**, 4167.
- 59 D. A. Zopf, S. J. Hollister, M. E. Nelson, R. G. Ohye and G. E. Green, *N. Engl. J. Med.*, 2013, **368**, 2043.
- 60 C. Norotte, F. Marga, L. Niklason and G. Forgacs, *Biomaterials*, 2009, **30**, 5910.
- 61 M. Kamei, W. Brian Saunders, K. J. Bayless, L. Dye, G. E. Davis and B. M. Weinstein, *Nature*, 2006, **442**, 453.
- 62 J. Cadet, E. Sage and T. Douki, *Mutat. Res., Fundam. Mol. Mech. Mutagen.*, 2005, **571**, 3.
- 63 D. Kulms, E. Zeise, B. Pöppelmann and T. Schwarz, *Oncogene*, 2002, **21**, 5844.
- 64 D. K. Patel, A. H. Sakhaei, M. Layani, B. Zhang, Q. Ge and S. Magdassi, *Adv. Mater.*, 2017, **29**, 1606000.
- 65 T. Gissibl, S. Thiele, A. Herkommer and H. Giessen, *Nat. Photonics*, 2016, **10**, 554.
- 66 S. Lin, H. Yuk, T. Zhang, G. A. Parada, H. Koo, C. Yu and X. Zhao, *Adv. Mater.*, 2016, **28**, 4497.